GLOBAL SENSITIVITY ANALYSIS OF LIQUID HYDROGEN STORAGE DESIGN PARAMETERS FOR OVERALL AIRCRAFT DESIGN

Tim Burschyk[1], Benjamin Fröhler[1], Marko Alder[1] & Thomas Zill[1]

[1]German Aerospace Center (DLR), Institute of System Architectures in Aeronautics, Hamburg, Germany

Abstract

Hydrogen-powered aircraft have emerged as a promising solution to reduce aviation's climate impact. However, there are significant uncertainties in the current research landscape, particularly in the development of aviation specific liquid hydrogen technologies and their successful integration into aircraft systems. The performance assessment of these technologies relies heavily on assumptions about hydrogen storage and aircraft systems. To systematically address these assumptions and underlying uncertainties during the early design phase, this study employs a global sensitivity analysis for a hydrogen-powered short-range turboprop concept. Within the global sensitivity framework, design assumptions related to liquid hydrogen storage and integration are treated as independent input variables. Recognizing the complex nature of aircraft design, the study incorporates the interdependencies between the overall aircraft design and liquid hydrogen storage through an integrated process that includes aircraft and hydrogen subsystem sizing. Consequently, this approach allows for the identification of key factors influencing the liquid hydrogen system design and provides insight into their impact on critical aircraft performance metrics.

Keywords: Global Sensitivity Analysis, Aircraft Design, Technology Integration, Liquid Hydrogen

1. Introduction

Already today, aviation is responsible for a significant share of the anthropogenic greenhouse effect and with the expected growth in air traffic this trend is likely to intensify in future [1]. Minimizing the climate impact of aviation is a challenging task for the upcoming decades not only because of the rising demand, but also due to long development cycles for new technologies in aviation. The use of alternative energy carriers, such as sustainable aviation fuel (SAF) or liquid hydrogen (LH2), is seen as promising options to reduce aviation's impact on the anthropogenic greenhouse effect. They are capable of reducing net carbon dioxide (CO_2) emissions and additional non-CO_2 effects. In contrast to SAF-powered aircraft, the assessment of the potential of hydrogen-powered aircraft is difficult due to the lack of knowledge with regard to novel hydrogen technologies for aircraft applications. Although concepts for hydrogen-powered aircraft have been discussed for many decades [2, 3], only few experimental demonstrators were actually built [4]. Due to its immaturity of application for commercial aviation, it is important to consider design uncertainties in order to evaluate the potential of hydrogen-powered aircraft. A global sensitivity analysis (GSA) represents a comprehensive method to support this assessment, which is discussed in more detail in the following.

1.1 State of the art

Research efforts in aviation is currently focusing on the integration of LH2 as an energy carrier for future aircraft designs. However, due to the lack of experience with hydrogen technology for aircraft application, the conceptual aircraft design cannot rely on statistical data. To illustrate the wide range of assumptions for the design of hydrogen-powered aircraft, the gravimetric efficiency, or gravimetric index, of the hydrogen storage system is examined as a key performance indicator. Here, the gravimetric efficiency η_g is defined as

$$\eta_g = \frac{m_f}{m_f + m_t + m_s}, \quad (1)$$

where m_f represents the mass of the usable fuel, m_t the mass of the tank and m_s the mass of the systems, respectively. The concept of gravimetric efficiency is widely used in the design of hydrogen-powered aircraft and is a measure of how lightweight hydrogen can be stored. In literature, the gravimetric efficiency is either a result of the method used or directly an assumption of the hydrogen storage for the overall aircraft design. It depends on many parameters: choice of materials for the tank structure, operating procedures such as pressure levels, adjacent tank systems, distribution systems, insulation architecture, overall volume and shape, as well as technology forecasts for future entry into service. Also, the comparability is limited due to different accounting of the mass fractions of Equation 1. Therefore, a wide range of the gravimetric efficiency values can be obtained from various studies in literature: ADLER et al. [5] provides an interval of literature values between 0.3 and 0.9. In the study of large hydrogen-powered aircraft for various ranges, a gravimetric efficiency of 0.30 - 0.85 is used by HUETE et al. [6]. A roadmap for hydrogen technologies from the year 2026 up to 2050 is presented in the FLY ZERO REPORT [7]. In this report, the LH2 tank gravimetric efficiency of 0.47 (0.64) is estimated for a regional aircraft and 0.58 (0.75) for a long range aircraft in 2026 (2050). The range of the values of these examples underlines the uncertainty designing novel hydrogen technologies for aircraft applications.

1.2 Objectives

Conceptual aircraft design methods cannot rely on statistical data for modeling hydrogen specific technologies and depend on physics-based approaches in connection with a wide range of assumptions. Acknowledging the dependency of hydrogen-powered aircraft performance on technology assumptions, a transparent design process is needed to support the evaluation of hydrogen-powered aircraft concepts. Conducting a GSA of LH2 storage design parameters improves the understanding of the design and solution space in different ways. First, highly influential or interacting parameters can be identified and their impact on the overall aircraft design are quantified. Secondly, the dependency of the design space on assumptions is estimated helping to create a common understanding for the risks and potential of hydrogen-powered aircraft. Furthermore, the results can be used to formulate research priorities that will pave the way for future technology developments.

2. Design aspects of liquid hydrogen storage

The design aspects of LH2 storage for aircraft application are manifold. They are driven by safety, certification, performance and economic requirements and, uniquely for the commercial aviation sector, the cryogenic properties of LH2. In order to provide an non-exhaustive overview, the aspects can be clustered in several subgroups: aircraft operation, aircraft integration, structural and fuel system specific aspects. In Figure 1 some LH2 storage specific design aspects are illustrated conceptually. Based on these aspects, aggregated design parameters can be derived in Chapter 4.2 to cover the design space for this study.

2.1 Aircraft operation aspects

Considering the entire life cycle of aircraft, operations is the dominating part alongside production/acquisition and end of life due to its intense and long usage [8]. In aircraft operations, a distinction can be made between flight operations and maintenance operations. Each operation phase entails some specific design aspects for LH2 storage systems, which are explained in more detail below.

2.1.1 Flight operations

The operation of aircraft with LH2 as energy carrier must be established in an economically competitive environment in order to represent a viable alternative. It is therefore reasonable to assume that turnaround performance needs to be comparable to that of conventional aircraft. Due to cryogenic character of LH2, the refueling operation differs from the operation with kerosene. For the refueling process, purging of air and the chill down of the refueling pipes are mandatory before the transfer of LH2 can be started. In order to compensate the delay of the additional steps of the refilling process,

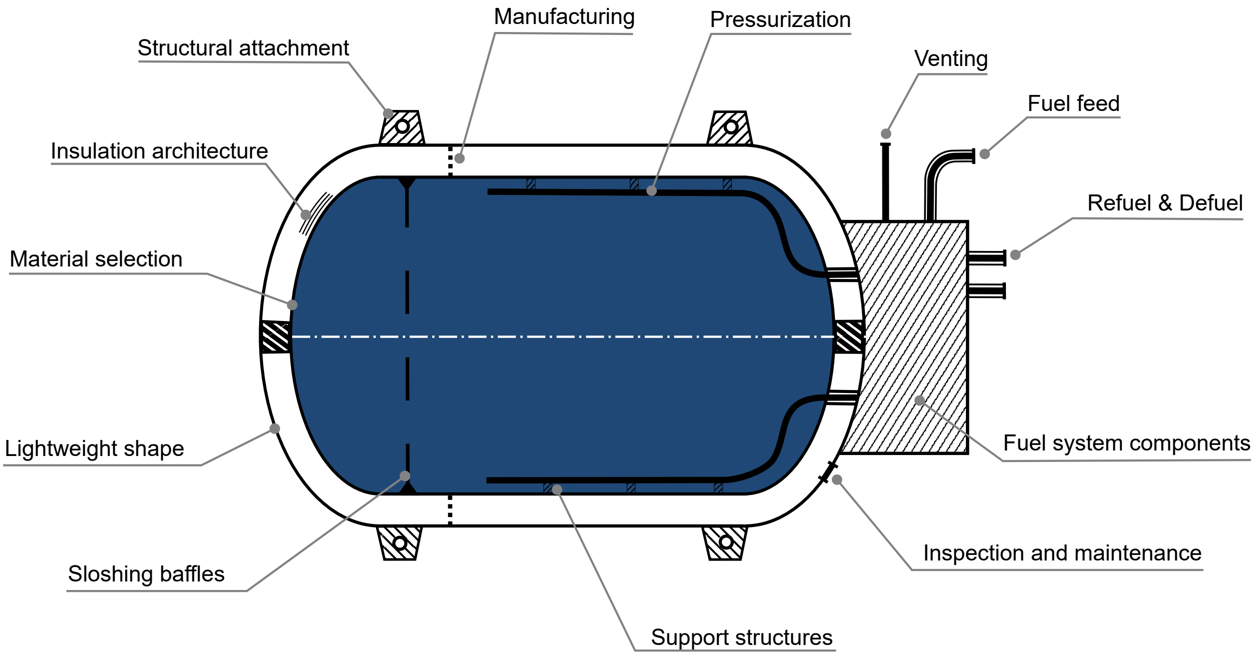

Figure 1 – Conceptual illustration of some design aspects of LH2 storage for aircraft application.

the transfer rate of liquid hydrogen could be increased, resulting in a similar performance according to MANGOLD et al. [9].
Another crucial aspect of the turnaround procedure is the ability to carry out simultaneous activities during refueling. Activities, such as deplaning, boarding, catering, cleaning or loading cargo, depend partly on each other and should be optimized to minimize the turnaround time. Referring to the FLY ZERO REPORT [7], the execution of these activities depends on the safety exclusion zone of the hydrogen refueling process. This separation distance needs to be minimized by technical means.
Moreover, the dormancy time of the LH2 storage is regarded as an important design aspect [7, 10]. In order to gain flexibility for ground handling and to reduce boil-off losses, a high dormancy time is desirable. On the contrary, a high dormancy time requires either a well-insulated tank or a high venting pressure, both leading to increased storage weights. Therefore, a balance of the dormancy time requirement has to be found. Some literature suggests dormancy times between 3 to 12 hours, also depending on the condition before and after the flight [7, 10, 11].

2.1.2 Maintenance operations

Besides the flight operation, the aircraft maintenance strategy plays an important role for the definition of design requirements. In case of the LH2 storage system, one key aspect is the ability to exchange the storage tank. This requirement drives many aspects concerning aircraft integration, but also the life expectancy target (e.g. thermal or mechanical load cycles) of the storage tank. In the case of LH2 tank exchange, WEHRSPOHN et al. [12] suggests to couple the exchange process with the heavy maintenance visit of the aircraft, which occurs every 6 - 12 years depending on the aircraft size and utilization [13]. Therefore, the frequency of the scheduled exchange and the infrastructure of the maintenance shop drive the requirements of the tank exchange mechanism.
Besides the possible exchange of the tank, additional dedicated maintenance tasks of the cryogenic hydrogen system have to be performed. These tasks include for example visual inspection of the tank's structural integrity, functional checks of valves or removal of parts for in-shop maintenance [14]. In order to complete these maintenance tasks, the accessibility to the systems has to be guaranteed. Consequently, sufficient system spacing and access panels are required from a maintenance perspective.

2.2 Aircraft configuration aspects

The hydrogen storage system closely interacts with the overall aircraft configuration. Due to its size and volumetric constraints, the optimal integration is challenging. Therefore, the several possible storage locations and their implications are discussed in the following. Moreover, the interactions between the aircraft power provider and the hydrogen fuel system are outlined in this chapter.

2.2.1 Storage location

Due to the low volumetric energy density of liquid hydrogen and the special requirements for the shape of the cryogenic pressure storage tanks, the storage cannot be accommodated in the wings, as is the case with kerosene-powered aircraft. Therefore, various options for a conventional tube & wing designs are being discussed, looking for suitable locations in terms of safety, operability and flight performance. A much-studied configuration is the integration of the storage tanks into the fuselage, as the tanks can utilize the fuselage width from a geometric perspective, minimizing the surface-to-volume ratio. In this configuration, the storage tanks could be integrated behind the rear pressure bulkhead. With increasing fuel requirements for longer ranges, a configuration with tanks in front of and behind the cabin is often chosen as this allows better control of the center of gravity shift. The uncertainty for this configuration is the unclear cockpit accessibility, which is required from CS-25.772(c) [15]. Other storage locations include the tank above the fuselage or as pods under the wings, each with its own specific challenges and benefits [10, 16, 17].
From a certification perspective, a survivable crash condition, hydrogen leakage or uncontrolled engine failure are some of the driving forces behind the requirements for the storage location. In the case of a storage tank integrated into the fuselage, the need for a crash structure and the space required by the deformation path might limit the maximum diameter of the storage tank within the fuselage. In addition, the relative position of the tank and the fuel consumer determines the routing of the fuel system. To reduce the risk of certification problems, pressurized compartments such as the cabin might be excluded. For routing the fuel line outside the fuselage, BREWER [3] proposes a fairing for the fuel lines on the top of the fuselage. This protects the fuel lines, but this increases the wetted area and the weight of the fuselage structure.

2.2.2 Aircraft power provider

In order to convert the chemical energy of the hydrogen and supply the power to generate thrust, two different concepts are mostly mentioned in literature: direct combustion, or the use of fuel cells. These power providers have different scaling laws, making the choice dependent on the aircraft size. Based on a review of various concepts from industry and literature, ADLER et al. [5] states that fuel cells are used only for an aircraft size up to small turboprops. The efficiency of fuel cells is rather independent of the power class, such that also small power classes achieve high efficiencies. In contrast, the combustion in gas-turbines achieves very high mass specific power values and high efficiencies at high power classes, making them a more suitable choice for lager aircraft.
The aircraft power provider sets the requirements for the hydrogen supply and therefore the hydrogen fuel system. The requirements of fuel cells and direct combustion differ with respect to pressure and temperature. Because fuel cells operate at a lower pressure (e.g. SCHRÖDER et al. estimates 1.6 bar as optimal stack pressure for an airborne PEM system [18]), the fuel supply might be driven using only the differential pressure of the storage tank. Consequently, no pump is required for this approach and the fuel system architecture might use the excess heat of the fuel cell or other components of the electric power train to condition the hydrogen, shown by VIETZE et al. [11]. For direct combustion, the required pressure must be high enough to inject the hydrogen in the combustion chamber. Considering the overall pressure ratio of modern turbo-machinery, a high-pressure pump is needed to supply the hydrogen [3, 10]. Regarding the conditioning of the hydrogen, GÖRTZ et al. [19] discuss possibilities to make use of low temperatures of the hydrogen in the cycle process to improve the specific fuel consumption up to 4.6 % depending on the concept. Summarizing the effects of the aircraft power provider, the close interaction with the fuel supply system and the storage pressure becomes apparent.

2.3 Structural aspects

This chapter provides an overview of the structural aspects of the tank design. The different options for materials, tank shapes and suspension concepts are discussed. Based on the different solutions, the areas of uncertainty are highlighted and possible design consequences are drawn.

2.3.1 Materials

Typical structural materials for storing liquid hydrogen are stainless steel, aluminum alloys or composite materials [20]. Due to their high strength-to-weight ratio, aluminum alloys and composite materials are commonly proposed for the application in the aviation sector [5]. The materials are exposed to hydrogen and cryogenic conditions influencing their thermal and mechanical properties. There is limited knowledge about the fatigue strength for such environments for the use within the commercial aviation sector. BREWER [3] proposes an estimate of reduced design stress for the aluminum alloy 2219-T851, but to the authors' knowledge, no fatigue estimate for composite materials under such conditions is publicly available. Another aspect is the gas tightness of the storage compartment. The permeability of the materials, especially for composites without a liner, is discussed as fundamental issue [21]. Moreover, manufacturing related aspects influence the design. These include the properties of joints, welds, bond lines, openings, and inhomogeneous materials (e.g. caused by ply gaps of composites). To account for these uncertainties, safety factors might be adjusted, different design criteria and failure modes considered, or additional tank layers, such as liners added.

2.3.2 Tank shape

The shape of the tank must meet several objectives. It must withstand internal overpressure (and external overpressure for vacuum-insulated tanks) while being lightweight, minimizing the surface-to-volume ratio to ensure good insulation, and being well to manufacture. Therefore, tank shapes consist typically of cylindrical parts, conical segments and domes, as can be observed by various examples [3, 22, 16, 23]. For torispherical domes and conical segments from metallic materials structural reinforcements are necessary and calculation rules can be obtained from [24]. In case of winded composite tanks for the application of storing LH2, FREUND et al. [23] shows, that the mass of the domes can be minimized substantially by using an isotensoid shape. The optimization of the domes seeks a good compromise between a low weight and a compact design, as discussed by [3]. Uncertainties for mass penalties occur for conformal tank design due to their suboptimal pressure vessel shape [5]. WINNEFELD et al. [25] estimates high mass penalties for non-circular cylindrical sections. Considering these effects, strongly deviating shapes from the typical pressure vessel design might have a strong influence on the mass.

2.3.3 Suspension concepts

The design aspect of suspension concepts is strongly coupled with the aircraft integration covered in Chapter 2.2 and maintenance requirements discussed in Chapter 2.1.2. Some studies propose a direct integration of the tank structure into the airframe structure, known as integral tanks [3, 22]. Following this approach, potential mass savings and a better volumetric utilization must be weighed against more complex structural loads and reduced maintainability. In contrast, non-integral tanks need a suspension to the airframe and therefore have the possibility to decouple the loads, which simplifies the definition of the sizing cases of the tank structures. BREWER [3] describes a four-point tank support system similar to the ones used for mounting aircraft engines. In case of vacuum insulated tanks suspension concepts need to be defined not only from the aircraft structure to the outer jacket, but also from the outer jacket to the inner vessel. This design needs to be optimized for opposing criteria: minimal mass and minimal heat leakage. This influences the integration space needed (between vacuum jacket and pressure vessel, as well as airframe and vacuum jacket) since longer supports can reduce heat conduction into the tank.

Another aspect affecting the suspensions is the crash-worthiness of the concept. As mentioned in Chapter 2.2.1, a crash structure and enough space for deformation need to be included for a fuselage integrated storage tank. Moreover, the suspensions need to carry the inertial loads of the tank in order to avoid a failure of the structure. The load carrying path might be reinforced including the airframe and stiffeners. Ultimately, the suspension concept design remains a trade-off between lightweight construction, compact design, thermal conduction and maintainability.

2.4 Fuel system aspects

Beside the storage tank itself, the hydrogen fuel system is necessary to provide all functions for operation. It consists of an engine fuel delivery system, fueling and defueling system, fuel transfer system and pressurization and venting system [3]. The fuel system architecture depends on the aircraft power provider as discussed in Chapter 2.2.2. Therefore, this Chapter is dedicated to specific fuel system components, insulation types of the storage compartment, sloshing and their possible implications.

2.4.1 System components

The systems components used for the configuration depend on the fuel system architecture, which itself needs to fulfill the requirements of the aircraft power provider. Within the scope of this paper, few components of a pump-driven fuel architecture are discussed in this chapter. BREWER [3] proposes to use a boost pump to supply fuel to the engines and pressurize the LH2 to avoid multi-phase flow in the fuel lines. One design aspect for a cryogenic low-pressure pump is the required "net positive suction pressure" (NPSP), which describes the pressure difference between the pump inlet pressure and the saturation pressure at the actual temperature of the liquid. To avoid cavitation, either an appropriate height of the liquid, a pressurization of the storage, or a supercharger at the inlet is needed [20]. Moreover, the reliability and lifetime of such pumps is an often cited challenge [5].

Another aspect is the design of fuel lines for LH2 supply. Therefore, pressure drop, heat input and specific line mass need to be considered beside safety, fabrication and maintainability [3]. For the line assembly and line materials different options can be obtained from literature. As for the insulation of the storage tank, the insulation type might be based on foam or vacuum with radiation shielding. BREWER [3] suggests stainless steel for the inner line material, a foam insulation and an outer aluminum jacket. In the CRYOPLANE REPORT [10], double walled composite fuel lines are discussed, stressing the low mass, rapid chill down, high strength, tolerance to handling damage and inherent vibration damping as possible advantages.

In addition to lines and pumps, numerous components require special attention for the application to a cryogenic fuel system. Some of these components are valves and their actuation, sensing equipment, leak detection, sealing, joints, bracketry and supports [7, 10]. The demanded reliability of the system might require more redundant components as for conventional systems. Their integration, e.g. in a vacuum system compartment for thermal insulation and hydrogen leak detection, could cause the need for additional sealed containers. Summarizing the system components, the estimated performance of such components under development and their integration imposes a high uncertainty with respect to system mass and space allocation requirements.

2.4.2 Insulation

The insulation system needs to fulfill the best compromise between mass, compactness, insulation quality and cost, to meet all safety and performance requirements defined by the operation aspects, such as the dormancy time (Chapter 2.1.1). Among many types of insulation systems and materials, the insulation based on closed-cell foam and double walled vacuum with multi-layer insulation are commonly considered [5]. Foam, as lightweight insulation material, is well-established for space applications [3, 7, 26]. For its application to aviation systems, the durability, performance deterioration and maintainability are areas of uncertainty. Compared to closed-cell foam, multi-layer vacuum insulation has a much lower heat leakage, but is heavier (requires an outer vacuum jacket) and is more complex. In case of vacuum rupture, the insulation capacity is rapidly being lost [3], leading to the discussion to add a thin foam layer to obtain a minimal insulation for this failure case. The design of the insulation influences the mass of the tank and the geometric dimensions not only directly, but also indirectly, through the thermodynamic behavior of the tank, and the sizing of the fuel system.

2.4.3 Sloshing

Sloshing is a phenomenon that can be described as the movement of a liquid within a partially filled enclosure. For conventional aircraft fuel tanks, the loads on the tank walls and the effects on stability and control due to the shift of the center of gravity have been investigated. If LH2 is used as fuel, an additional effect must be considered: In cryogenic liquids, evaporation and condensation effects can lead to pressure fluctuations or mixing of different thermal layers, which can affect the fuel extraction system [27]. MILLS et. al [28] proposes slosh baffles to inhibit the movement of the fuel. The internal structures of the tank require a larger tank volume, increase the structural mass and are complex to integrate depending on the manufacturing process. In addition, the ability of pressure control systems could affect the maximum allowable pressure to ensure reliable fuel extraction even with pressure fluctuations. The uncertainty of pump inlet conditions due to the mixing of different thermal layers of the fluid could be addressed by the amount of unusable fuel considered in the design.

3. Methodology

This chapter provides an overview of the combined hydrogen storage and aircraft concept sizing, the approach for the GSA, as well as the surrogate model framework as a prerequisite for the GSA.

3.1 Combined aircraft and system design

The sizing of both the overall aircraft and the liquid hydrogen storage tanks is achieved through a unified process executed by the workflow-driven integration platform RCE (Remote Component Environment) [29]. The aircraft design process (ADP) includes disciplinary processes linked in a convergence loop that address component mass estimation [30, 31], mission performance calculation, low-speed performance [32] and the LH2 storage and system sizing process. These sub-processes are interconnected by DLR's standardized data schema CPACS [33], which facilitates consistent information exchange and storage of aircraft data. The ADP is initialized using the DLR's in-house conceptual aircraft sizing and design synthesis tool openAD [34], which is a handbook-based tool consisting mainly of empirical and semi-empirical methods [35, 36, 37, 38].
Figure 2 illustrates the procedure of the LH2 storage and system sizing. This sub-process calculates the thermodynamic performance, geometry, and mass of the hydrogen storage systems [39]. This information is then integrated into the overall aircraft design process. The detailed framework of this integrated approach is thoroughly described by BURSCHYK et al. [40]. This methodology not only facilitates the sizing of hydrogen-powered aircraft concepts, but also extends its capabilities to accommodate variable input parameters for LH2 storage modeling.

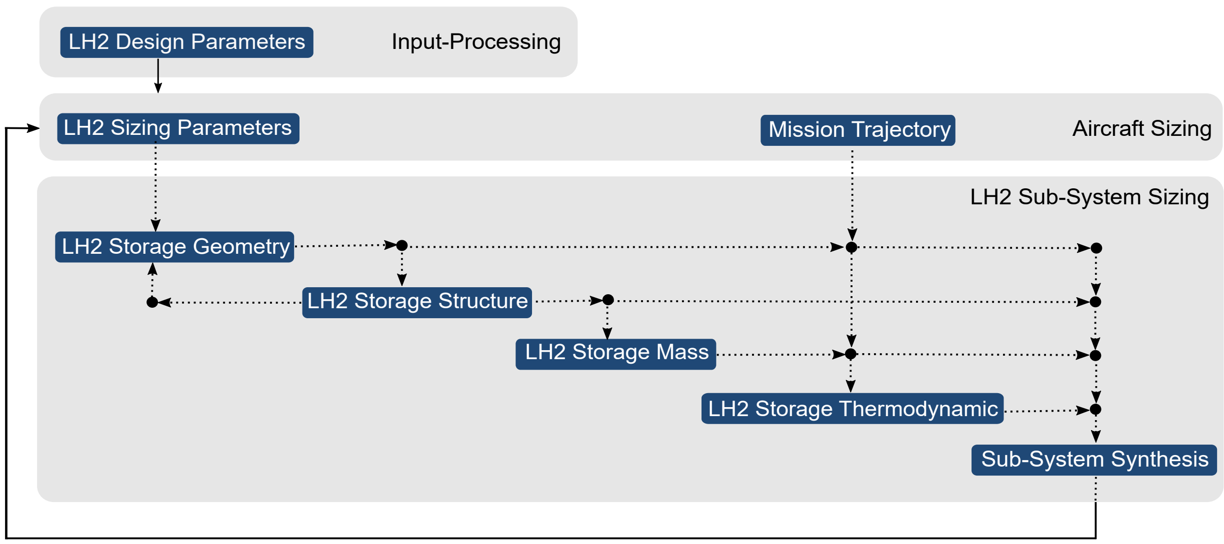

Figure 2 – LH2 storage and system sizing sub-process, adapted from [40].

3.2 Global sensitivity analysis

The described aircraft and system sizing methodology in Chapter 3.1results in a single deterministic design solution. To improve the informative value of the study and to identify highly influential parameters, a sensitivity analysis is carried out for the combined aircraft and system sizing methodology. A sensitivity analysis provides insights in "how the uncertainty in the output of a model can be apportioned to different sources of uncertainty in the model input" [41]. The way of conducting such a sensitivity analysis can be differentiated between local and global. A local sensitivity analysis uses the model's response of varying a single, or few parameters, around a normal value to estimate the model's behavior regarding this parameter. Although quite intuitive, this method is limited to linear models and cannot account for interacting parameters. In contrast, GSA covers the whole design space instead of focusing on a single design point at the price of computational cost. Furthermore, the GSA is able to provide a ranking of the most influential input parameters with respect to the model's output. According to RAZAVI et al. [42], several techniques have been developed of which the most prominent can be grouped in the following categories: derivative-based, variance-based and response surface-assisted. ALDER et al. [43] compared these approaches for the application of conceptual aircraft design. As stated in this previous study, the variance-based approach offers highly precise sensitivity measures and, therefore, is selected for conducting the GSA in this study for aircraft design. The analysis of variance (ANOVA) gains information on the global influence of input factors on their contribution to the variance of the model output [41]. The so called Sobol' method [44] combines the ANOVA with a high-dimensional model representation (HDMR) making the method applicable to Monte-Carlo-based algorithms.

The Sobol' method is outlined in the following, using the nomenclature according to SALTELLI et al. [45]: For a generic model $Y = f(X)$ the expression with a nonnull range of variation of the model input sets $X = (X_1, X_2, .., X_k)$ reads

$$Y = f(X_1, X_2, .., X_k). \tag{2}$$

This expression, if integrable over the k-dimensional unit hypercube, can be expanded into terms of increasing dimensions

$$f(x) = f_0 + \sum_i f_i + \sum_i \sum_{i<j} f_{ij} + ... + f_{12...k}, \tag{3}$$

where the terms are only functions of their index factors and result in a finite number of terms. In general, the HDMR is not unique and the terms could be represented by an infinite number of choices. But, if each term of the expansion has zero mean (i.e. are orthogonal), it can be shown, that these terms can be uniquely represented using conditional expectations:

$$f_0 = E(Y) \tag{4}$$

$$f_i = E(Y|X_i) - E(Y) \tag{5}$$

$$f_{ij} = E(Y|X_i, X_j) - f_i - f_j - E(Y) \tag{6}$$

The conditional expectations $E(Y|X_i)$ can be calculated empirically and their variation across X_i serve as indicators measuring their importance. Therefore, the ANOVA-HDMR decomposition is introduced as a final step in order to obtain a qualitative sensitivity measurement. The decomposition is obtained by square integrating the terms of Eq. (3) over the k-dimensional hypercube and resorting to

$$V(Y) = \sum_{i=1} V_i + \sum_{i=1} \sum_{i<j} V_{ij} + ... + V_{12...k}, \tag{7}$$

where $V(Y)$ represents the unconditional variance, $V_i = V[E(Y|X_i)]$ measures the variance with respect to X_i and $V_{ij} = V[E(Y|X_i, X_j)] - V_i - V_j$ is known as the joint effect of X_i and X_j, also called second-order effect. To obtain a relative quantification, the terms of Eq. (7) are divided by the unconditional variance, resulting in the first-order sensitivity index

$$S_{1_i} = \frac{V[E(Y|X_i)]}{V(Y)}, \tag{8}$$

and the second-order sensitivity index

$$S_{2_{ij}} = \frac{V[E(Y|X_i,X_j)] - V_i - V_j}{V(Y)}. \tag{9}$$

Additionally, to the first- and second-order sensitivity effects, a total sensitivity index S_{T_i} can be derived from the terms of Eq. (7), which accounts for the total influence of the factor X_i including first and all higher-order terms. By decomposing the output variance in main effect and residual [45], the total sensitivity index can be expressed with respect to all factors except one (i.e. $X_{\sim i}$)

$$S_{\mathrm{T}_i} = 1 - \frac{V[E(Y|X_{\sim i})}{V(Y)}, \tag{10}$$

facilitating the computation. A significant difference between S_{1_i} and S_{T_i} is a sign for an important interaction of this factor. If S_{T_i} is close to zero, the factor might be fixed to a deterministic value within its range without influencing the output variance. Applied to the use case of integrating liquid hydrogen as aviation fuel, these sensitivity measures increase the understanding of its design parameters and determine important, interacting, and non-influential factors in a systematic way.

3.3 Framework for sensitivity studies

The general process to derive global sensitivity measures is illustrated in Figure 3. The process starts with the literature study on the technologies been investigated. In addition, expert knowledge can be consulted for deeper insides into the different aspects and underlying uncertainties. Subsequently, global sensitivity measures can be determined. Using the Sobol' method to derive variance-based global sensitivity measures requires a high number of function evaluations. Therefore, a surrogate model of the combined aircraft and system design is generated in order to decrease the computational effort. For the construction of surrogate models, the German Aerospace Center (DLR) develops the Python library "Surrogate Modeling for Aero Data Toolbox in Python" (SMARTy) [46, 47, 48], which provides capabilities to model surrogates of complex aircraft systems. The construction of the surrogate model is performed using the framework introduced by the authors' previous work [49]. The framework creates the design of experiment with the required samples and triggers the aircraft design process in RCE (see Chapter 3.1). The advantage of the surrogate framework is the robust execution of each sample in RCE and the automatic tracking of sample convergence and removal of failed process executions. First, test data are generated to validate the surrogate model using a Latin hypercube sampling strategy. Then the parameter space is discretized using a Sobol' sampling strategy for the surrogate training data. As final step to refine the surrogate model, the method of maximum likelihood is applied based on error estimation to identify parameter regions where the highest improvement by additional sampling is expected. For the surrogate model, the regression algorithm is based on the Gaussian process, which is well established in the literature and implemented in the SMARTy toolbox [50] with the Kriging method.

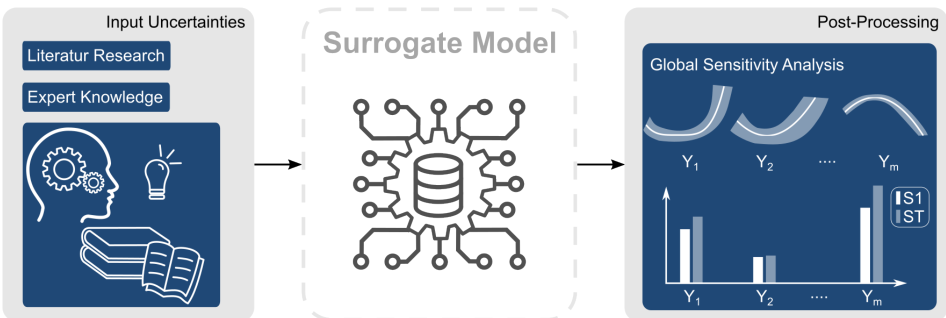

Figure 3 – Framework for global sensitivity studies [49].

Within the post-processing, the surrogate model is used for GSA. This involves defining the problem description that was established during the initial literature review phase. The problem description includes identifying influential parameters, specifying their probability density functions (PDFs), and selecting the parameter to be investigated. Using the Python library SALib [51, 52], the input set is re-sampled and the surrogate model is used for model evaluation. This allows the determination of sensitivity measures such as sensitivity indices, which are previously outlined in Chapter 3.2.

4. Results and discussion

The GSA, outlined in Chapter 3.2, is applied to the hydrogen storage integration for a single-aisle aircraft concept. In Chapter 4.1, the specific aircraft concept and hydrogen architecture is described. Based on this concept and the hydrogen storage design aspects discussed in Chapter 2, design parameters and their intervals are formulated in order to define the design space. This design space is covered by a suitable surrogate model and further explored in Chapter 4.3.1. Therefore, sensitivity indices are calculated for different input parameter distributions to identify highly influential parameters. The results are concluded by the global effects of the input parameter variations on overall aircraft key characteristics.

4.1 Aircraft and hydrogen storage concept

The single-aisle aircraft concept in Figure 4 serves as use-case for the GSA of LH2 storage design parameters. It is derived from a DLR interpretation of the Airbus A321neo [53] and adopted tor a turboprop concept for an assumed technology level of the year 2040. Capable of transporting 250 passengers over maximal 1500 NM, it could cover a large share of the short-range market segment. This concept is equipped with two propellers powered by gas turbines. To allow the integration of the propellers, a mild gull-wing with wing-mounted main landing-gears is designed. To reduce the interactions between the propeller wake and the horizontal stabilizers, a T-tail empennage is chosen. The turboprop configuration is selected for this study, because it offers significant potential to reduce climate impact [54]. Some of its top-level aircraft requirements are listed in Table 1 and more information on the aircraft concept and LH2 storage details can be obtained from BURSCHYK et al. [40].

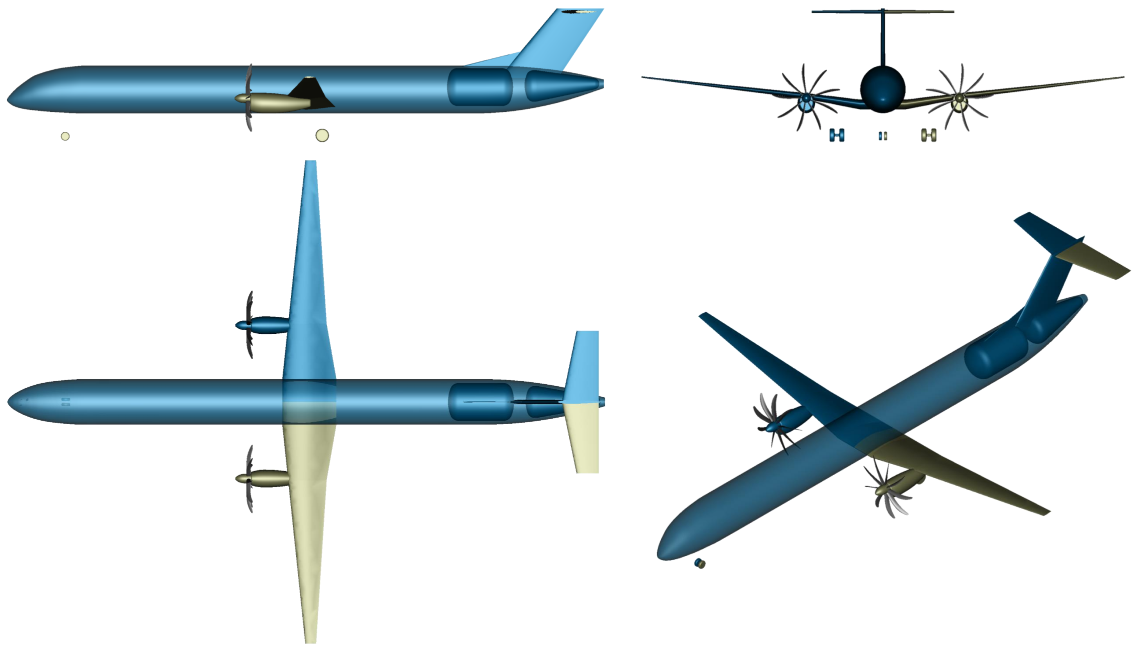

Figure 4 – Hydrogen-powered short-range turboprop concept.

As boundary condition for this study, the hydrogen storage integration concept is specified with respect so some regards. The two liquid hydrogen tanks are integrated as non-integral tanks into the rear of the fuselage, which is a well suited location in terms of aerodynamic performance and ground based operability [17]. MLI serves as insulation architecture, because of the superior insulation performance and safety advantages with respect to hydrogen leakage and detection. Since the aircraft is powered by turboprop engines, the fuel system is based on a pump-driven architecture based on the architecture presented by BREWER [3]. For the structural material of the LH2 pressure vessel and the vacuum jacket aluminum alloy is selected. These design decisions remain unchanged while conducting the sensitivity analysis.

Table 1 – Brief overview of some top-level aircraft requirements.

Parameters	Unit	Value
Design Range	NM	1500
Design Passenger Capacity	-	250
Mass per Passenger	kg	95
Design Cruise Mach Number	-	0.66
Foldable wing span limit (Box limit)	m	42 (36)

4.2 Design space definition

The hydrogen-powered short-range turboprop concept is used as starting point for the design space generation. In Chapter 4.2.1, design parameters are chosen specifically for this configuration and their interval boundaries are defined. Based on these parameters, a surrogate model is generated with the framework explained in Chapter 3.3. The suitability of the surrogate model is shown in Chapter 4.2.2, providing different error indications.

4.2.1 Design parameters

Including various aspects regarding aircraft operation and integration, as well as structural and system design, aggregated parameters can be defined from an overall aircraft design perspective. For the assessment on overall aircraft design level, the resulting mass, volume and performance of the subsystem are required. Therefore, eight parameters are selected to represent these metrics. They are either defined as range of physical values or as scaling factors applied on components. Figure 5 provides an overview of the selected parameters.

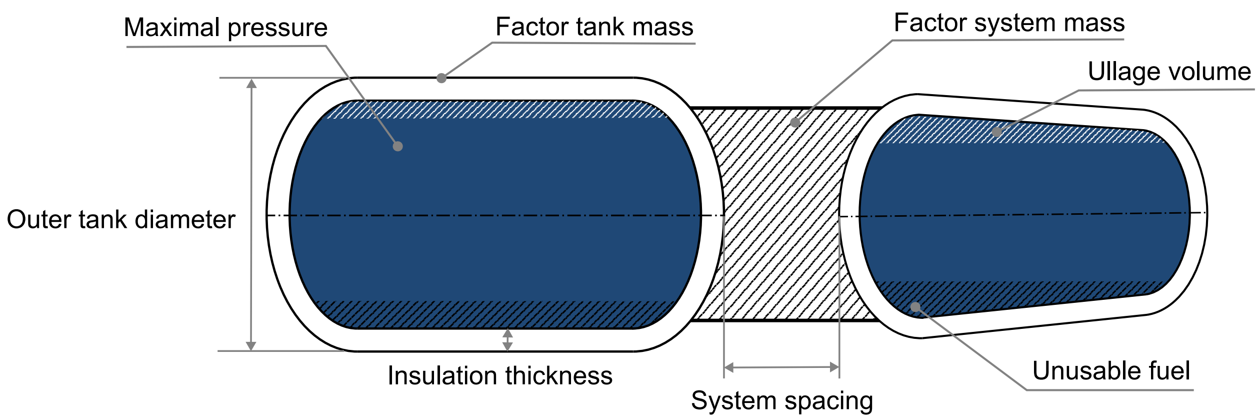

Figure 5 – Illustration of LH2 tank design parameters.

The definition of the **maximum pressure** of the storage vessel is impacted by many design aspects, for example the dormancy time requirement for normal operation, the time of emergency venting in case of insulation failure, the ability to control the pressure, or the NPSP of the low-pressure pump. According to ADLER et al. [5], the maximal pressure in literature is indicated somewhere in between 1.5 - 3.0 bar(a). For a pressure-driven fuel system maximal pressure values of up to 10.0 bar(a) can be found in VIETZE et al. [11]. When applying a vacuum insulation with a pump-driven fuel system, the values in literature are lower such as 1.45 bar(a) [3] and 2.1 bar(a) [55]. These studies included the dormancy time as requirement, but did not consider the NPSP of the boost pump as possible requirement driver. Therefore, the boundaries of the design space for the maximum pressure are extended to 1.45 - 3.5 bar(a).

The **ullage volume** represents volumetric restrictions with in the storage compartment. It is influenced by the ability to control the pressure, the tank shape, inner structures, or safety requirements. For space application SUTTON et al. [56] provides a range of 3.0 - 10.0 % of the tank volume. HUETE et al. [55] consider an ullage of 5 %, while BREWER [3] assumes 2.0 %. Considering the extremes, the interval for the GSA is set to 2.0 - 10.0 %.

Also expressed as relative parameter, the **unusable fuel** is defined with respect to the maximal fuel mass. Similar to the ullage volume, geometric circumstances can cause trapped fuel resulting in geometric unusable fuel. Also, the ability of the boost pump to deliver sub-cooled fluid up to a certain NPSP can influence the amount of unusable fuel. Especially, if the thermal stratification of the liquid is disturbed by sloshing events, the fuel delivery system still has to operate properly. BREWER [3] assumed a boost pump capable of processing saturated liquid and allowed 0.3 % unusable fuel in the preliminary design, whereas VERSTRAETE et al. [22] considered 3 % as unusable fuel. Under the circumstances described, the boundaries of the unusable fuel are expected to be between 2.0 - 10.0 %.

The **outer tank diameter** is restricted by the fuselage diameter for this non-integral tank configuration. Depending on suspension concepts, crash structure volume and space requirements for system spacing, only the available width of the fuselage can be used. The lower boundary is set, such that a maximal vertical space of about 1 m below the tank is allowed. Considering this estimate, the interval for the tank diameter ratio with respect to the fuselage is defined between 75 - 95 %.

Another geometrical parameter is the **insulation thickness**, defined as the space between the pressure vessel and the vacuum jacket. Together with thin additional foam layers, as depicted in [39], this parameter defines the thickness of the insulation system, which is assumed for dome and cylinder sections to be identical. The thickness depends on suspension and stiffener concepts, manufacturing processes and maintenance procedures, as well as material properties for expansion and contraction of the pressure vessel. In literature, values for the MLI or the vacuum space for the application to LH2 storage tanks in aviation can be obtained ranging from 5 mm [22] and 63.5 mm [3] to 127 mm [55]. Considering the total vacuum space and not only the thickness of the spacer and radiative blanket material, the boundaries for the insulation thickness are set to 0.05 - 0.20 m.

For the mass of the total tank and the fuel systems, factors are used to cover the extremely broad range of influencing design aspects. The **factor tank mass** tries to cover many structural aspects, e.g. the applied safety factor, margins for manufacturing and special requirements for integration of systems such as brackets, holes or stiffeners. The modeling of the tanks is physics-based with a reduced design stress [3] and a safety factor according to [24]. The safety factor for LH2 tanks is discussed by MITAL et al. [57], which outlines the uncertainty for the application under cryogenic conditions. The model includes margins for the suspension concept [39] depending on the structural mass of the tank component. Despite these margins, the influence of manufacturing and system integration is not considered within the modeling. Therefore, the range of boundaries for the factor of tank mass is set to 0.9 - 1.3 including the variation of safety factors, the margin for manufacturing and system integration and possible improvement in the structural design. The lower boundary might be achieved with a small safety factor and a minimal mass increase due to manufacturing, while the upper boundary represents a pessimistic combination of the influencing aspects.

The **factor system mass** is applied to the fuel system mass, which is modeled analog to BREWER [3]. In contrast to the fuel system presented in the CRYOPLANE REPORT [10] the system does not feature active or passive tanks. Also, the fuel lines are insulated with closed-cell foam and therefore are lightweight. To acknowledge the uncertainty of the fuel system mass, the interval of the factor is defined between 1.0 - 2.0 rating the mass of the baseline system as optimistic.

Specific to this configuration, the **system spacing** defines the distance between the tanks and is affected by the fuel system volume requirements, maintenance needs and possible tank exchange mechanisms. With the objective to minimize the space, the interval is set to 0.5 - 2.0 m.

All combined, these parameters form the design space for the described configuration. They are aggregated from an overall aircraft design point of view and their intervals represent an estimate specific to the chosen architecture. The parameters and their intervals are summarized in Table 2. In order to compare the results of the GSA relative to each other, a hydrogen-powered short-range turboprop concept of a previous study [40] serves as LH2 baseline. The underlying assumptions for the LH2 baseline are likewise shown in Table 2.

Table 2 – Interval definition of design space parameters.

Parameters	Unit	Interval	LH2 Baseline [40]	Remark
Factor system mass	-	1.0 - 2.0	1.0	Scaling of system mass
Outer tank diameter	%	75.0 - 95.0	92.0	w.r.t. fuselage diameter
System spacing	m	0.5 - 2.0	0.5	Distance between tanks
Factor tank mass	-	0.9 - 1.3	1.1	Scaling of tank mass
Unusable fuel	%	2.0 - 10.0	10.0	w.r.t. max. fuel mass
Ullage volume	%	2.0 - 10.0	5.0	w.r.t. tank volume
Insulation thickness	m	0.05 - 0.20	0.05	Vacuum spacing
Maximal pressure	bar(a)	1.45 - 3.5	2.0	Structural sizing condition

4.2.2 Surrogate model

Once the surrogate model is constructed based on the outlined parameters in Table 2, it represents the aircraft design combined with the LH2 system sizing. For the surrogate model generation, the intervals of the design space are extended to ensure a good quality within the boundaries. For the generation of the surrogate model 160 training samples are used. In Table 3, main aircraft and system characteristics as output of the surrogate model are validated against test samples of the workflow. Therefore, the maximum take-off mass (MTOM), the operating empty mass (OEM), the block fuel (BF), lift-over-drag (L/D), the thrust specific fuel consumption (TSFC), the gravimetric efficiency η_g and the volumetric efficiency η_v (introduced in Chapter 4.3.1) are analyzed with different error indicators. The mean squared error (RMS Error), the mean absolute error, maximal error and R^2 provide a comprehensive overview of the quality of the surrogate. Considering $R^2 > 0.978$ for all main aircraft characteristics, the surrogate provides sufficient accuracy to conduct the GSA. Due to the good agreement with the test samples of the workflow, the additional uncertainty introduced by the surrogate is neglected in the GSA.

Table 3 – Error scores for main aircraft characteristics.

Parameters	Unit	RMS Error	Mean Abs. Error	Max. Error	R^2
MTOM	kg	99.6	81.9	201.7	0.998
OEM	kg	97.6	79.7	194.9	0.998
BF (des. mission)	kg	3.70	3.07	6.92	0.997
L/D (des. mission, mid cruise)	-	0.023	0.019	0.056	0.982
TSFC (des. mission, mid cruise)	kg/Ns	1.30e-09	1.029e-09	3.22e-09	0.983
η_g	%	0.53	0.43	1.00	0.978
η_v	%	0.46	0.38	0.80	0.986

4.3 Global sensitivity analysis

The results of the GSA are presented in this chapter. First, the design space of the previous defined parameters is explored with respect to aircraft and system evaluation characteristics. Based on the results, different input distributions of design parameters are compared to each other to identify highly influential parameters for each distribution and to display the effect of the variance of the input parameters to the final overall aircraft design.

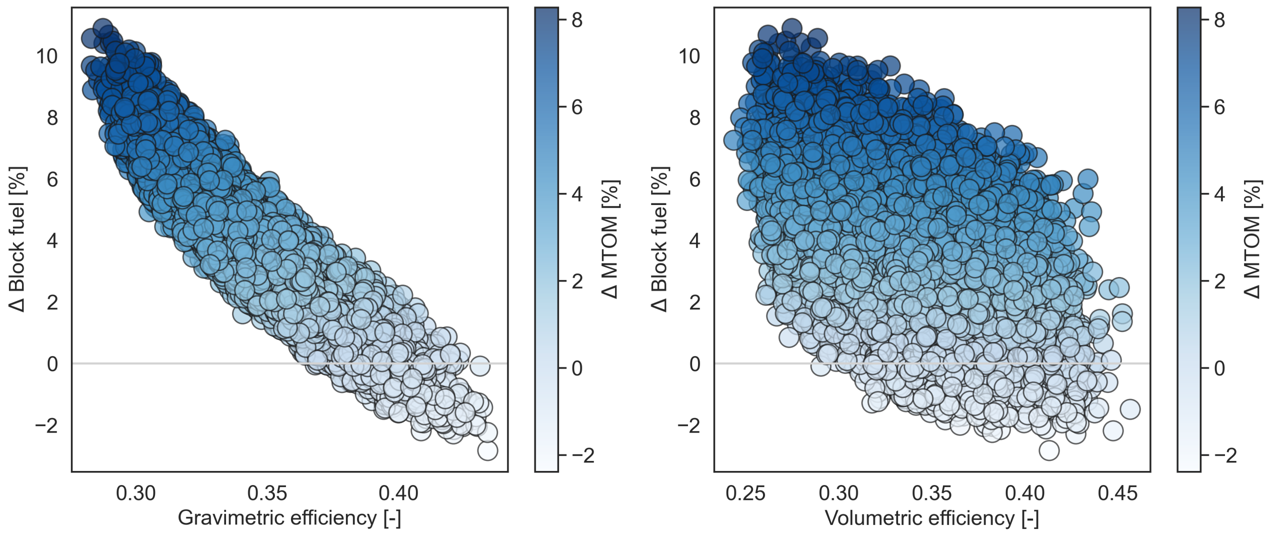

(a) (b)

Figure 6 – Design space exploration with uniform input distributions.

4.3.1 Design space exploration

A design space exploration provides valuable insights in the overall system behavior, system boundaries and general trends. In Figure 6a and Figure 6b, the design space for the parameter intervals in Table 2 is visualized. This scatter plot is generated using the surrogate model and Monte-Carlo sampling of a uniform distribution of the design parameters. The relative aircraft evaluation characteristics Δ Block fuel and Δ MTOM refer to the LH2 baseline and are plotted against LH2 storage specific metrics: the gravimetric efficiency and the volumetric efficiency. In analogy to gravimetric efficiency in Equation 1, the volumetric efficiency is defined as

$$\eta_{\mathrm{v}} = \frac{V_{\mathrm{f}}}{V_{\mathrm{c}}}, \tag{11}$$

where V_{f} is the volume of the LH2 fuel at saturation conditions of 1 bar(a) and V_{c} is the total volume of the compartment enclosed by the pressure bulkhead and the aircraft skin in the rear. It has to be noted, that the definition of the volumetric efficiency depends on the integration configuration and does not provide a universal characteristic. However, for this study, it provides a valuable measure of the geometrical integration quality for this configuration. Moreover, the design space of this configuration is not restricted by the fuselage length. Therefore, an unfavorable combination of design parameter values could result in a fuselage length of more than 54 m, which would interfere with ground operability. Nevertheless, in order to provide trends and sensitivities, these sample points are not excluded from the design space.

Within the interval of the design space, the gravimetric efficiency varies from 0.28 - 0.44 resulting in a deviation of -3 % block fuel up to +11 % compared to the LH2 baseline. The low dispersion of the Monte-Carlo samples and the clear trend line emphasize the strong correlation of gravimetric efficiency with the deviation in block fuel and MTOM, respectively. In Figure 6b, the samples are plotted against the volumetric efficiency, which provides a more scattered distribution. The volumetric efficiency varies between 0.25 - 0.45, meaning that less than half of the volume behind the pressure bulkhead is occupied by the volume of LH2 for this integration configuration. The overall trend for the volumetric efficiency indicates a minor influence on the evaluation parameters due to the wider spread of the samples.

4.3.2 Sensitivity indices

The GSA aims to apportion the uncertainty of the output to different sources of uncertainty in its inputs. Applying the so-called Sobol' Method, the sensitivity of each input can be represented using sensitivity indices, which is outlined in Chapter 3.2. In Figure 7, the first-order sensitivity indices S_{1_i} are shown for key aircraft and system performance indicators. The total sensitivity indices S_{T_i} are very similar to S_{1_i} indicating a weak interaction between the design parameters within the model. The sensitivity indices S_{1_i} in Figure 7 are calculated using a uniform distribution of the intervals in Table 2. Before discussing the sensitivities of the design parameters on aircraft level, the influence on the gravimetric efficiency η_g and volumetric efficiency η_v is outlined. The gravimetric efficiency η_g is mainly influenced by the maximal pressure, the tank mass scaling, the unusable fuel and the system mass scaling. In contrast, the volumetric efficiency η_v is mainly sensible to the tank diameter ratio, the insulation thickness and the system spacing. The results on aircraft level can be interpreted as weighted combination of these two system level indicators. The sensitivity indices for MTOM and OEM show similar trends following the main influential parameters of η_g, since they reflect the LH2 system masses directly including their snowball effects. The aerodynamic performance indicator L/D is mainly sensible to the maximal pressure and the tank mass scaling, as well as the insulation thickness and the tank diameter ratio. Due to the influence of the insulation thickness and the tank diameter ratio on the wetted area, their effect is reflected in the aerodynamic performance. The BF and TSFC indicate similar dependencies on the design parameters. They are dominated by the maximal pressure and the tank mass scaling.

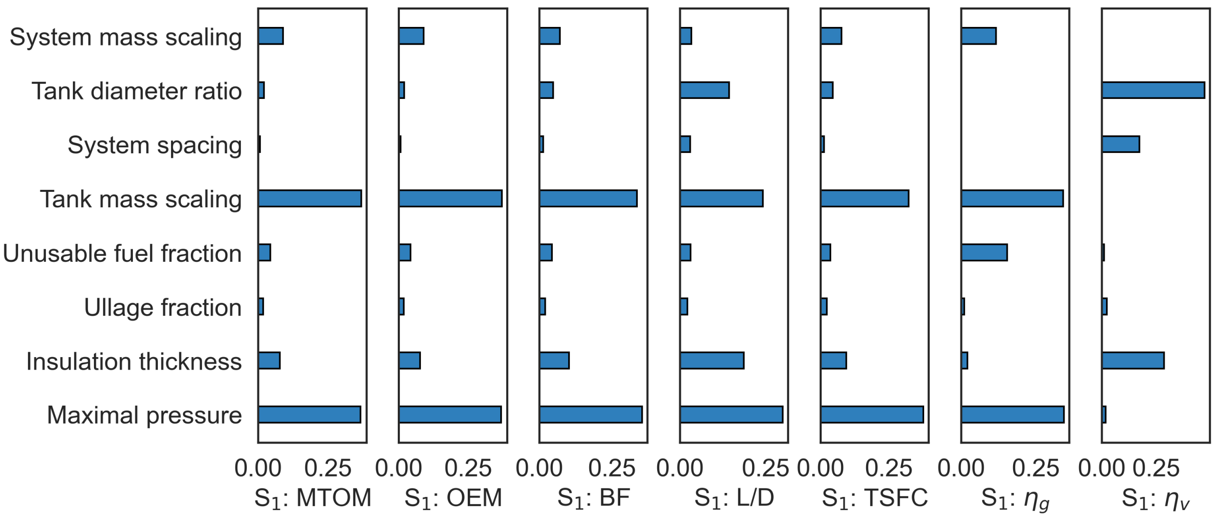

Figure 7 – Sensitivity indices S_{1_i} of key performance indicators using a uniform input distribution.

Figure 7 provides insights of the first-order sensitivity indices for a uniform distribution of the parameter intervals, meaning that each value of the input interval is equally probable. In Table 4, alternative input distributions are defined for some of the parameters. They are formulated as truncated normal distributions comprising of interval boundaries of the design space, mean values μ and standard deviations σ. Using this distribution, the boundaries are ranked less probable while the mean value as more probable. The input distributions are refined for five parameters based on literature and engineering judgment. The outer tank diameter as ratio of the fuselage diameter is not expected to sit tight on the frames, nor leave space for about 1 m below the tank resulting in massive penalties for the volumetric efficiency. Therefore, a mean value of 83.0 % is estimated providing a margin for system integration. The mean of the ullage fraction is set to 5 % following the assumption of Huete et al. [55]. Likewise, the unusable fuel fraction is ranked. The insulation thickness is set in the manner, that the literature values [3, 55] are considered within the standard deviation interval. For the maximal pressure, the optimized value of 2.1 bar(a) [55] is chosen as mean value resulting in an unsymmetrical distribution. The input distributions of the remaining parameters are kept uniformly distributed.

Table 4 – Refined alternative parameter input distribution definition.

Parameters	Unit	Interval	Distribution	μ	σ
Factor system mass	-	0.5 - 2.0	unif.	-	-
Outer tank diameter	%	75.0 - 95.0	trunc. normal	83.0	5.0
System spacing	m	0.5 - 2.0	unif.	-	-
Factor tank mass	-	0.9 - 1.3	unif.	-	-
Unusable fuel	%	2.0 - 10.0	trunc. normal	5.0	2.0
Ullage volume	%	2.0 - 10.0	trunc. normal	5.0	2.0
Insulation thickness	m	0.05 - 0.20	trunc. normal	0.09	0.04
Maximal pressure	bar(a)	1.5 - 3.5	trunc. normal	2.1	0.5

Using the refined input distributions summarized in Table 4, the sensitivity indices S_{1_i} of key performance indicators are depicted in Figure 8. They provide a similar trend compared to the previously discussed sensitivity indices with uniform input distributions in Figure 7. Main differences are the reduced S_1 values for the maximal pressure reflecting the more concentrated input distribution. As consequence of the decrease of the input variance for the truncated normal distributed parameters, the uniformly distributed parameters gain relative importance. Therefore, the tank mass scaling dominates all key performance indicators except of η_v and also the influence of the system mass scaling is ranked higher. This alternative input parameter distribution definition showcases the ability of the method to reflect the effect of different assumptions on the respective sensitivity measures.

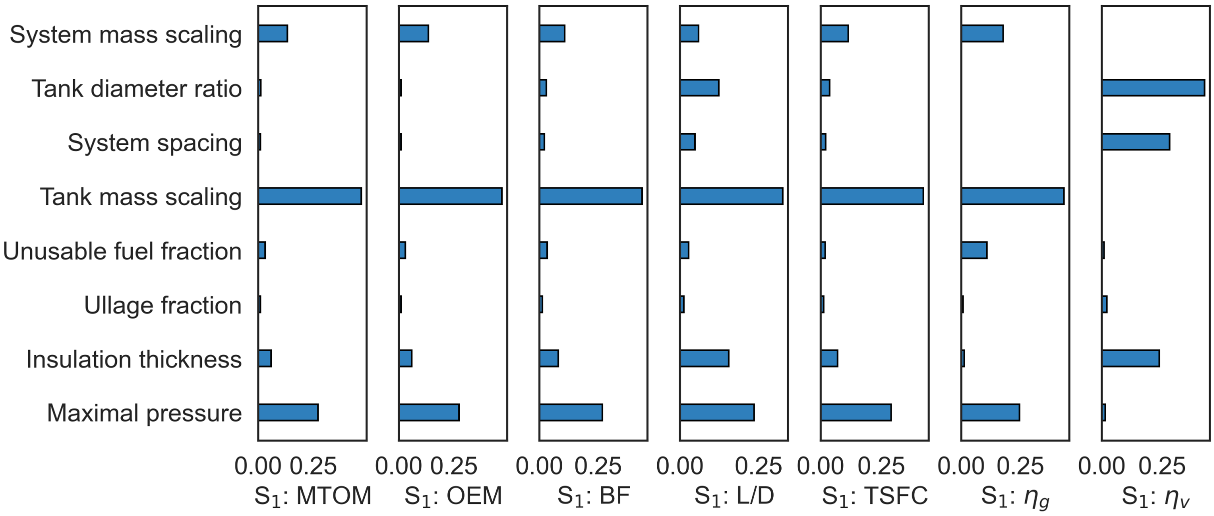

Figure 8 – Sensitivity indices S_{1_i} of key performance indicators using the input distributions of Table 4

4.3.3 Total output variance

The previously discussed sensitivity indices indicate the relative influence of the different input parameters on the output variance. The total output variance of the key performance characteristics is shown in Figure 9 as box-and-whisker diagram. The box of the diagram is bounded by the lower and upper quartile of the output data samples meaning that 50 % of the samples are represented by the box. The whiskers are based on the 1.5 value of the interquartile range excluding outliers. Figure 9a shows the relative difference of aircraft key performance indicators with respect to the LH2 baseline [40]. The figure is generated using the refined input parameter distributions of Table 4. Compared to the LH2 baseline, the median of the MTOM is estimated 1.6 % higher. Likewise, the medians for OEM and block fuel are estimated about 2 % higher and the values of the LH2 baseline are located below the lower quartile. The value of the median for L/D is -0.8 % indicating the worse quality of the aerodynamic performance compared to the LH2 baseline and its design parameter assumptions.

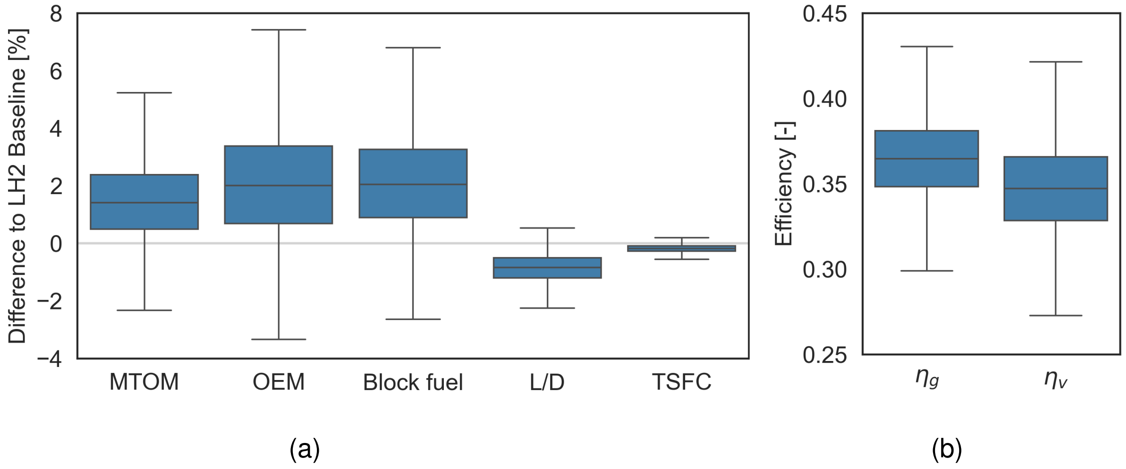

Figure 9 – Total output variance of key performance indicators as result of the GSA.

The median of the TSFC improved minimally as a result of the engine sizing. The dispersion of the resulting key performance indicators shows different behavior. While the L/D and the TSFC are less dispersed, the data sets of MTOM, OEM and block fuel are more spread. The whiskers of the block fuel are between -2.5 - 7.1 %, which underlines the influence of the assumption selection for the LH2 storage and system design parameters on the overall aircraft design.

In Figure 9b, the dispersion of the values for η_g and η_v are displayed. Defined to measure the volumetric integration quality for this study, the median of η_v is 0.35 and the whisker boundaries are 0.28 and 0.42. For η_g, the values for the lower and the upper quartile are 0.35 and 0.38, respectively. The whisker boundaries are located between 0.30 - 0.43. These estimated values are at the lower spectrum of the range for η_g compared to various publications [3, 7, 22, 5, 6]. It must be noted, that the comparability is limited by the chosen LH2 storage and integration concept, the total tank volume, the material selection, the assumed technology advancement and the bookkeeping of η_g. Nevertheless, the spread of η_g illustrates the strong dependency of the underlying assumptions being prerequisite to preliminary aircraft design.

5. Conclusion

This study examines the dependence of hydrogen aircraft design on LH2 storage parameters. Given the uncertainties of LH2 technologies for aircraft applications, modeling cannot not rely on deterministic approaches based on statistical data. Therefore, physics-based models in combination with design assumptions are used for the aircraft design. Addressing this issue, a variance-based GSA is performed to systematically identify highly influential design parameters and to assess their effect on aircraft performance indicators. In order to provide suitable design parameters and their respective intervals for the GSA, different aspects of the LH2 storage design are based on literature data. These aspects include the aircraft operation and aircraft configuration, as well as structural and fuel system specific issues. A hydrogen-powered short-range turboprop concept with vacuum insulated aluminum tanks serves as use-case for this study. This aircraft concept is designed by an integrated process, that includes the interdependencies of aircraft and hydrogen subsystem sizing. The design process results in a single deterministic aircraft concept. In order to make it applicable to the variance-based, probabilistic GSA, a surrogate model is generated representing the design space of the selected design parameters. Providing each design parameter with an input distribution, their sensitivities can be assessed and the uncertainty of the aircraft indicators with respect to LH2 storage parameters can be quantified.

The GSA identified the maximum pressure, the tank mass scaling and the system mass scaling as the most influential parameters on η_g measured by the first-order sensitivity index. The tank diameter, defined as the ratio to the fuselage diameter, the system spacing and the insulation thickness were decisive for η_v. For the use-case aircraft concept, half of the sample data of the GSA indicate η_g in the range of 35 - 38 %, while the extremes of η_g in the design space are in between 28 to 44 %.

The influencing parameters at overall aircraft level can be interpreted as a weighted combination of η_g and η_v. MTOM and OEM follow the trend of η_g, while L/D is also influenced by the parameters that are decisive for η_v. Compared to the LH2 baseline of a previous study, the median of the design mission block fuel is estimated 2 % higher, with half of the data in a range of 0.8 - 3.2 % additional block fuel and the limits of the design space located at -3 % and 11 %, respectively. This comparison exemplifies the better understanding of the assumptions which are made on the LH2 storage in preliminary aircraft design. Adding this output distribution to the deterministic result, the subsequent assessment of hydrogen-powered aircraft can be improved.
Future studies could apply this method to different aircraft configurations and LH2 storage architectures in order to compare the design spaces and support decision making. Also, the sensitivity indices for aircraft configurations of different size, such as mid- or long-range configuration are of interest.

6. Contact Author Email Address

Tim Burschyk
German Aerospace Center (DLR)
Institute of System Architectures in Aeronautics, Hamburg, Germany
mailto: tim.burschyk@dlr.de

7. Copyright Statement

References

[1] Volker Grewe, Arvind Gangoli Rao, Tomas Grönstedt, Carlos Xisto, Florian Linke, Joris Melkert, Jan Middel, Barbara Ohlenforst, Simon Blakey, Simon Christie, Sigrun Matthes, and Katrin Dahlmann. Evaluating the climate impact of aviation emission scenarios towards the paris agreement including covid-19 effects. *Nature communications*, 12(1):3841, 2021.

[2] Abe Silverstein and Eldon. W. Hall. Liquid hydrogen as a jet fuel for high-altitude aircraft.

[3] G. Daniel Brewer. *Hydrogen aircraft technology*. CRC Press, Boca Raton, 1991.

[4] V. Sosounov and V. Orlov. Experimental turbofan using liquid hydrogen and liquid natural gas as fuel. In *26th Joint Propulsion Conference*, Reston, Virigina, 1990. American Institute of Aeronautics and Astronautics.

[5] Eytan J. Adler and Joaquim R.R.A. Martins. Hydrogen-powered aircraft: Fundamental concepts, key technologies, and environmental impacts. *Progress in Aerospace Sciences*, 141:100922, 2023.

[6] J. Huete, D. Nalianda, and P. Pilidis. Impact of tank gravimetric efficiency on propulsion system integration for a first-generation hydrogen civil airliner. *The Aeronautical Journal*, 126(1302):1324–1332, 2022.

[7] Aerospace Technology Institute. Flyzero - cryogenic-hydrogen-fuel-system-and-storage-roadmap-report: Fzo-ppn-com-0027.

[8] Paul Clark. *Buying the big jets: Fleet planning for airlines*. Routledge Taylor & Francis Group, London and New York, third edition edition, 2017.

[9] Jonas Mangold, Daniel Silberhorn, Nicolas Moebs, Niclas Dzikus, Julian Hoelzen, Thomas Zill, and Andreas Strohmayer. Refueling of lh2 aircraft—assessment of turnaround procedures and aircraft design implication. *Energies*, 15(7):2475, 2022.

[10] Airbus Deutschland GmbH. Liquid hydrogen fueled aircraft - system analysis: Final technical report: Cryoplane. 2003.

[11] Marco Vietze and Stefan Weiland. System analysis and requirements derivation of a hydrogen-electric aircraft powertrain. *International Journal of Hydrogen Energy*, 2022.

[12] Jennifer Wehrspohn, Antonia Rahn, Veatriki Papantoni, Daniel Silberhorn, Tim Burschyk, Matthias Schröder, Florian Linke, Katrin Dahlmann, Markus Kühlen, Kai Wicke, and Gerko Wende. A detailed and comparative economic analysis of hybrid-electric aircraft concepts considering environmental as-

sessment factors. In *AIAA AVIATION 2022 Forum*, Reston, Virginia, 06272022. American Institute of Aeronautics and Astronautics.

[13] Shannon P Ackert. Basics of aircraft maintenance programs for financiers. *Evaluation & insights of commercial aircraft maintenance programs*, 10, 2010.

[14] Robert Meissner, Patrick Sieb, Eric Wollenhaupt, Stefan Haberkorn, Kai Wicke, and Gerko Wende. Towards climate-neutral aviation: Assessment of maintenance requirements for airborne hydrogen storage and distribution systems. *International Journal of Hydrogen Energy*, 48(75):29367–29390, 2023.

[15] European Union Aviation Safety Agency. Certification specifications and acceptable means of compliance for large aeroplanes (cs-25) amendment 27: Cs-25.

[16] Florian M. Troeltsch, Marc Engelmann, Anna E. Scholz, Fabian Peter, Jochen Kaiser, and Mirko Hornung. Hydrogen powered long haul aircraft with minimized climate impact. In *AIAA AVIATION 2020 FORUM*, Reston, Virginia, 2020. American Institute of Aeronautics and Astronautics.

[17] D. Silberhorn, G. Atanasov, J-N. Walther, and T. Zill. Assessment of hydrogen fuel tank integration at aircraft level. *German Aerospace Congress*, 2019.

[18] M. Schröder, F. Becker, J. Kallo, and C. Gentner. Optimal operating conditions of pem fuel cells in commercial aircraft. *International Journal of Hydrogen Energy*, 2021.

[19] Alexander Görtz and Daniel Silberhorn. Thermodynamic potential of turbofan engines with direct combustion of hydrogen. In *33rd Congress of the International Council of the Aeronautical Sciences (ICAS 2022)*, Bonn, Germany, 2022. International Council of Aeronautical Sciences (ICAS).

[20] Walter Peschka. *Liquid Hydrogen: Fuel of the Future*. Springer Vienna, Vienna, 1992.

[21] Michael Robinson, Jeffrey Eichinger, and Scott Johnson. Hydrogen permeability requirements and testing for reusable launch vehicle tanks. In *43rd AIAA/ASME/ASCE/AHS/ASC Structures, Structural Dynamics, and Materials Conference*, Reston, Virigina, 2002. American Institute of Aeronautics and Astronautics.

[22] D. Verstraete, P. Hendrick, P. Pilidis, and K. Ramsden. Hydrogen fuel tanks for subsonic transport aircraft. *International Journal of Hydrogen Energy*, 35(20):11085–11098, 2010.

[23] Sebastian Freund and Felipe Franzoni. Automated liquid hydrogen tank design optimization using filament winding simulation and subsequent comparison with aluminium vessels. In *DLRK 2022*, September 2022.

[24] *AD 2000-Regelwerk: Taschenbuch-Ausgabe 2016*. Handbuch Technische Regeln. Beuth Verlag GmbH, Berlin, 10. auflage edition, 2017.

[25] Christopher Winnefeld, Thomas Kadyk, Boris Bensmann, Ulrike Krewer, and Richard Hanke-Rauschenbach. Modelling and designing cryogenic hydrogen tanks for future aircraft applications. *Energies*, 11(1):105, 2018.

[26] J. E. Fesmire, B. E. Coffman, B. J. Meneghelli, and K. W. Heckle. Spray-on foam insulations for launch vehicle cryogenic tanks. *Cryogenics*, 52(4-6):251–261, 2012.

[27] Francesco Saltari, Marco Pizzoli, Mario Tindaro Migliorino, Antonello Binni, Giuliano Coppotelli, Franco Mastroddi, Tiziano Pagliaroli, Fabio Del Duchetto, Francesco Gambioli, Ramon Abarca, and Henning Scheufler. Experimental investigations on the sloshing-induced pressure drop in tanks for hydrogen-powered aircraft. In *AIAA SCITECH 2024 Forum*, Reston, Virginia, 2024. American Institute of Aeronautics and Astronautics.

[28] Gary L. Mills, Brian Buchholtz, and Al Olsen. Design, fabrication and testing of a liquid hydrogen fuel tank for a long duration aircraft. In *AIP Conference Proceedings 2012*, pages 773–780. 2012.

[29] Brigitte Boden, Jan Flink, Niklas Först, Robert Mischke, Kathrin Schaffert, Alexander Weinert, Annika Wohlan, and Andreas Schreiber. Rce: An integration environment for engineering and science. *SoftwareX*, 15:100759, 2021.

[30] P. Balack, T. Hecken, M. Petsch, G. Atanasov, D. Silberhorn, and B. Nagel. Semi-physical method for the mass estimation of fuselages carrying liquid hydrogen fuel tanks in conceptual aircraft design.

[31] Tobias Hecken, Philip Balack, Michael Petsch, and David Zerbst. Conceptual loads assessment of aircraft with fuselage integrated liquid hydrogen tank. In *German Aerospace Congress (DLRK)*, Dresden, Germany, September 2022.

[32] B. Fröhler, C. Hesse, G. Atanasov, and P. Wassink. Disciplinary sub-processes to assess low-speed performance and noise characteristics within an aircraft design environment.

[33] M. Alder, E. Moerland, J. Jepsen, and Björn Nagel. Recent advances in establishing a common language for aircraft design with cpacs. *Aerospace Europe Conference 2020*, 2020.

[34] Sebastian Wöhler, Georgi Atanasov, Daniel Silberhorn, Benjamin Fröhler, and Thomas Zill. Preliminary aircraft design within a multidisciplinary and multifidelity design environment. *Aerospace Europe Conference 2020*, 2020.

[35] Egbert Torenbeek. *Advanced aircraft design: Conceptual design, analysis, and optimization of subsonic*

civil airplanes. Aerospace series. Wiley, Chichester West Sussex United Kingdom, 2013.

[36] Egbert Torenbeek. *Advanced aircraft design: Conceptual design, technology and optimization of subsonic civil airplanes*. Aerospace Ser. John Wiley & Sons Incorporated, New York, online-ausg edition, 2013.

[37] Douglas P. Wells, Bryce L. Horvath, and Linwood A. McCullers. The flight optimization system weights estimation method, 2017.

[38] Daniel P. Raymer. *Aircraft design: A conceptual approach*. AIAA education series. American Institute of Aeronautics and Astronautics Inc, Reston, VA, sixth edition edition, 2018.

[39] Tim Burschyk, Yannic Cabac, Daniel Silberhorn, Brigitte Boden, and Björn Nagel. Liquid hydrogen storage design trades for a short-range aircraft concept. *CEAS Aeronautical Journal*, 2023.

[40] Tim Burschyk, Daniel Silberhorn, Jennifer Wehrspohn, Markus Kühlen, and Thomas Zill. Scenario-based implications of liquid hydrogen storage tank insulation quality for a short-range aircraft concept. In *AIAA AVIATION 2023 Forum*, Reston, Virginia, 2023. American Institute of Aeronautics and Astronautics.

[41] Andrea Saltelli, Ksenia Aleksankina, William Becker, Pamela Fennell, Federico Ferretti, Niels Holst, Sushan Li, and Qiongli Wu. Why so many published sensitivity analyses are false: A systematic review of sensitivity analysis practices. *Environmental Modelling & Software*, 114:29–39, 2019.

[42] Saman Razavi, Anthony Jakeman, Andrea Saltelli, Clémentine Prieur, Bertrand Iooss, Emanuele Borgonovo, Elmar Plischke, Samuele Lo Piano, Takuya Iwanaga, William Becker, Stefano Tarantola, Joseph H.A. Guillaume, John Jakeman, Hoshin Gupta, Nicola Melillo, Giovanni Rabitti, Vincent Chabridon, Qingyun Duan, Xifu Sun, Stefán Smith, Razi Sheikholeslami, Nasim Hosseini, Masoud Asadzadeh, Arnald Puy, Sergei Kucherenko, and Holger R. Maier. The future of sensitivity analysis: An essential discipline for systems modeling and policy support. *Environmental Modelling & Software*, 137:104954, 2021.

[43] Marko Alder, Tawfiq Ahmed, Benjamin Fröhler, and Anna Skopnik. Assessment of techniques for global sensitivity analyses in conceptual aircraft design. In *AIAA AVIATION 2023 Forum*, Reston, Virginia, 2023. American Institute of Aeronautics and Astronautics.

[44] I. M. Sobol'. Sensitivity estimates for nonlinear mathematical models. *Mathematical Modelling and Computational Experiments*, (4):407–414, 1993.

[45] Andrea Saltelli, Marco Ratto, Andres Terry, Francesca Campolongo, Jessica Cariboni, Debora Gatelli, Michaela Saisana, and Stefano Tarantola. *Global sensitivity analysis: The Primer*. Wiley, Chichester, West Sussex, 2008.

[46] Zhong-Hua Han and Stefan Görtz. Hierarchical kriging model for variable-fidelity surrogate modeling. *AIAA Journal*, 50(9):1885–1896, sep 2012.

[47] T. Franz, R. Zimmermann, S. Görtz, and N. Karcher. Interpolation-based reduced-order modelling for steady transonic flows via manifold learning. *International Journal of Computational Fluid Dynamics*, 28(3-4):106–121, mar 2014.

[48] M. Ripepi, M. J. Verveld, N. W. Karcher, T. Franz, M. Abu-Zurayk, S. Görtz, and T. M. Kier. Reduced-order models for aerodynamic applications, loads and MDO. *CEAS Aeronautical Journal*, 9(1):171–193, feb 2018.

[49] Benjamin M. Fröhler, Marko Alder, Sebastian Wöhler, and Thomas Zill. Assessing uncertainties of an evolutionary baseline as benchmark of future aircraft designs. In *AIAA SCITECH 2024 Forum*, Reston, Virginia, 2024. American Institute of Aeronautics and Astronautics.

[50] Philipp Bekemeyer, Anna Bertram, Derrick A. Hines Chaves, Mateus Dias Ribeiro, Andrea Garbo, Anna Kiener, Christian Sabater, Mario Stradtner, Simon Wassing, Markus Widhalm, Stefan Goertz, Florian Jaeckel, Robert Hoppe, and Nils Hoffmann. Data-driven aerodynamic modeling using the dlr smarty toolbox. In *AIAA AVIATION 2022 Forum*, Reston, Virginia, 2022. American Institute of Aeronautics and Astronautics.

[51] Jon Herman and Will Usher. SALib: An open-source python library for sensitivity analysis. *The Journal of Open Source Software*, 2(9):97, jan 2017.

[52] Jon Herman and Will Usher. SALib module. `https://salib.readthedocs.io/en/latest/index.html`, [Online; accessed 22-Mai-2024].

[53] Airbus S.A.S. A321 Aircraft Characteristics Airport and Maintenance Planning. `https://www.airbus.com/sites/g/files/jlcbta136/files/2021-11/Airbus-Commercial-Aircraft-AC-A321.pdf`, [Online; accessed 31-Mai-2024].

[54] Georgi Atanasov, Jennifer Wehrspohn, Markus Kühlen, Daniel Silberhorn, Michael Kotzem, Katrin Dahlmann, Florian Linke, and Yannic Cabac. Short-medium-range turboprop-powered aircraft as a cost-efficient enabler for low climate impact. In *AIAA AVIATION 2023 Forum*, Reston, Virginia, 2023. American

Institute of Aeronautics and Astronautics.

[55] Jon Huete and Pericles Pilidis. Parametric study on tank integration for hydrogen civil aviation propulsion. *International Journal of Hydrogen Energy*, 46(74):37049–37062, 2021.

[56] George Sutton and Oscar Biblarz. Rocket propulsion elements. 2017.

[57] Subodh K. Mital, John Z. Gyekenyesi, Steven Arnold, Roy Sullivan, Jane Manderscheid, and Pappu Murthy. Review of current state of the art and key design issues with potential solutions for liquid hydrogen cryogenic storage tank structures for aircraft applications.